ACS APPLIED MATERIALS & INTERFACES

www.acsami.org

Research Article

Influence of Missing Linker Defects on the Thermal Conductivity of Metal–Organic Framework HKUST-1

Meiirbek Islamov, Hasan Babaei, and Christopher E. Wilmer*

Cite This: *ACS Appl. Mater. Interfaces* 2020, 12, 56172–56177

Read Online

ACCESS | Metrics & More | Article Recommendations | Supporting Information

ABSTRACT: Although metal–organic frameworks (MOFs) are promising materials for gas storage and separation applications, the heat released during the exothermic adsorption process can potentially negatively impact their practical utility. Thermal transport in MOFs has not been widely studied, and among the relatively few reports on the topic, MOFs have either been assumed to be defect free or the presence of defects was not discussed. However, defects naturally exist in MOFs and can also be introduced intentionally. Here, we investigate the effect of missing linker defects on the thermal conductivity of HKUST-1 using molecular dynamics (MDs) simulation and the Green–Kubo method. We found that missing linker defects, even at low concentrations, substantially reduce the thermal conductivity of HKUST-1. If not taken into account, the presence of defects could lead to significant discrepancies between experimentally measured and computationally predicted thermal conductivities.

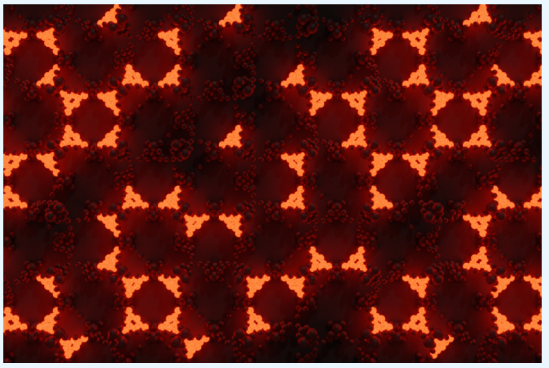

KEYWORDS: *metal–organic framework, thermal transport, missing linker defects, molecular dynamics simulation, Green–Kubo method*

INTRODUCTION

Metal–organic frameworks (MOFs) are highly porous, crystalline materials, which are constructed from metal nodes and organic ligands by self-assembly.[1,2] MOFs have attracted intense interest from industry and academia due to their wide application potential.[3] They have shown promise in gas storage, separation, sensing, and catalysis applications because of their extremely high surface area, porosity, and structural tunability.[4−16] A great variety of metal clusters and organic linkers are available for the design of MOFs with specific physical and chemical properties for the applications of need.

However, MOFs typically have low thermal conductivities (<2 W m^{-1} K^{-1}) because of their highly porous structure, which can impede the rapid removal of heat released during gas adsorption. Consequently, rapid adsorption in MOFs can lead to increase in temperature that in turn reduce their total adsorption capacity.[17] Despite the significance of heat transport in MOFs, relatively few studies have focused on this phenomenon.[18−26] Although in our own past work we have considered a range of factors that influence thermal conductivity in MOFs, including the effect of interpenetration,[27] pore size and shape,[28] and the presence of adsorbates,[29,30] we and others have always assumed perfect crystal structures without any defects.[31] Of course, MOFs are known to contain defects of various types, and over the last few years, defects in MOFs have attracted increasing attention.[32] Besides enabling a more complete understanding of thermal transport in MOFs, investigating the influence of defects could add an additional control knob for tailoring thermal conductivity, which can supplement other strategies previously described (e.g., pore size and shape, interpenetration).

In MOFs, vacancies related to either metal nodes or organic linkers form point defects.[31] Point defects naturally occur even in carefully synthesized pure MOF crystals. However, they can also be artificially introduced to modify the performance of MOFs (e.g., catalytic activity).[3] There are a few methods to introduce defects in MOFs on purpose: (a) using acid modulators to synthesize defective MOF structures with missing linkers;[33−35] (b) using inorganic acid for the postsynthetic treatment of MOFs;[36] and (c) generate defective MOFs with missing linkers by fast precipitation.[37]

There are a number of studies exist in the literature that investigated the impact of vacancies/defects on the thermal conductivity in other materials.[38−48] For instance, in perovskite oxides such as strontium-doped lanthanum cobaltite (LSCO) epitaxial films, oxygen vacancies remarkably reduced the thermal conductivity and showed a much higher impact on phonon scattering rate than mass disorder, which explains the close-to amorphous limit thermal conductivity of the epitaxial

Received: September 7, 2020
Accepted: November 23, 2020
Published: December 4, 2020

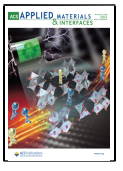

https://dx.doi.org/10.1021/acsami.0c16127
ACS Appl. Mater. Interfaces 2020, 12, 56172–56177

films with oxygen vacancies.[38] Also, the molecular dynamics (MDs) studies with carbon nanoribbons showed that the thermal conductivity dropped sharply at low defect concentrations (0.5−2.5%) and plateaued at higher concentrations.[39] Comparably, in 2D materials, such as graphene or graphene alternative, transition-metal dichalcogenides, namely $MoSe_2$, vacancy defects have been shown to be an effective strategy to suppress the thermal conductivity purposefully.[40,41] Specifically, at room temperature, 0.1% vacancies caused 95% reduction in graphene[40] and 5% vacancy caused ∼70% reduction of thermal conductivity in $MoSe_2$.[41] In crystalline silicon,[42] 1.5% vacancies led to 95% reduction, whereas in Boron arsenide (BAs),[43] which have been known to have an exceptionally high conductivity, 0.1% defect concentration resulted in 95% drop in the thermal conductivity.

In general, any compositional or structural disorder (e.g., mass impurity, heterogeneity) can be expected to significantly impact thermal conductivity. In most alloys, for example, having a 10−25% concentration of impurities (i.e., compositional disorder) leads to an order of magnitude reduction in the thermal conductivity.[44−46] Structural disorder in alloys has an even greater impact on reducing thermal conductivity.[47] In contrast, in zeolitic imidazolate frameworks (ZIFs), which are closely related to MOFs, glassy disordered structures showed higher thermal conductivities than their ordered crystalline counterparts.[48] This counterintuitive finding was ascribed to increased density and pore distortion but nevertheless highlights the complexity of thermal transport physics in highly porous materials. Although defects in MOFs introduce disorder that breaks their regular periodic arrangement, it is unknown what effects they would have on the thermal conductivity.

In this study, we focus on missing linker defects and their effect on the thermal conductivity of a widely studied MOF, $[Cu_3(btc)_2]$ (btc^{3-} = 1,3,5-benzenetricarboxylate), also named HKUST-1 (Hong Kong University of Science and Technology).[49] Namely, we report our investigation on the effect of missing linker defect concentration on the thermal conductivity of HKUST-1. We observed that the missing linker defects considerably decrease the thermal conductivity, even at lower defect densities. We believe that this is due to increased phonon-defect scattering in the HKUST-1 framework.

METHODOLOGY

We used molecular dynamics (MD) simulations and the equilibrium Green−Kubo method to calculate the thermal conductivity of the HKUST-1 system. The Green−Kubo formula is given by[50]

$$k_{ii} = \frac{V}{k_b T^2} \int_0^\infty \langle J_i(t) J_i(0) \rangle \mathrm{d}t, \quad i = x, \ y, \ z \tag{1}$$

where $\langle J_i(t) J_i(0) \rangle$ is the heat flux autocorrelation function (HCACF), which represents the strength of correlation between heat currents at time zero and time t, V is the volume of the supercell, k_b is the Boltzmann's constant, and T is temperature. The ith diagonal element of the thermal conductivity tensor is calculated by integrating the HCACF over the correlation time. Thermal conductivity is considered to have converged when the HCACF fluctuates around zero. For all structures, the thermal conductivity converged at around 30 ps of correlation time. Thus, to be consistent, for all structures including the pristine one, the thermal conductivity was calculated by averaging the conductivity values at 35−40 ps. For plots of the HCACF and thermal conductivity as a function of correlation time for each defect concentration, see the Supporting Information.

All thermal conductivity simulations were performed using the open-source MD simulation code LAMMPS.[51] The system consisted of a cubic 3 × 3 × 3 supercell with 7.9 nm in each dimension, which contained 16 848 atoms (see Figure 1). To investigate possible size effects, we performed thermal conductivity calculations using 2 × 2 × 2, 3 × 3 × 3, and 4 × 4 × 4 supercells of pristine HKUST-1. Since the thermal conductivity did not change appreciably for the 4 × 4 × 4 supercell case, we chose to use 3 × 3 × 3 simulation box sizes for all subsequent calculations. The system was large enough that manual removal of linkers using available molecular editors would be prohibitively difficult. So, to tackle this problem, we developed a Python script that detects and randomly deletes linkers (https://github.com/meiirbek-islamov/defects). The interatomic potential developed by Zhao et al.[52] was used to describe the interactions between HKUST-1 framework atoms. The timestep used was 0.5 fs in the MD simulation for all structures. Initially, the structures were run under canonical constant-volume-constant-temperature (NVT) ensemble at T = 300 K for 500 ps to set the temperature. Next, they were equilibrated under a microcanonical constant-volume-constant-energy (NVE) ensemble for 100 ps. Finally, the HCACF was calculated every five timesteps under NVE condition over 1 ns. A correlation length of 5 × 10^5 timestep was used in the HCACF. For each defect structures, to sufficiently sample the phase space, the thermal conductivity was obtained by averaging 16 independent simulations with random initial velocity distributions. Periodic boundary conditions were applied in all directions.

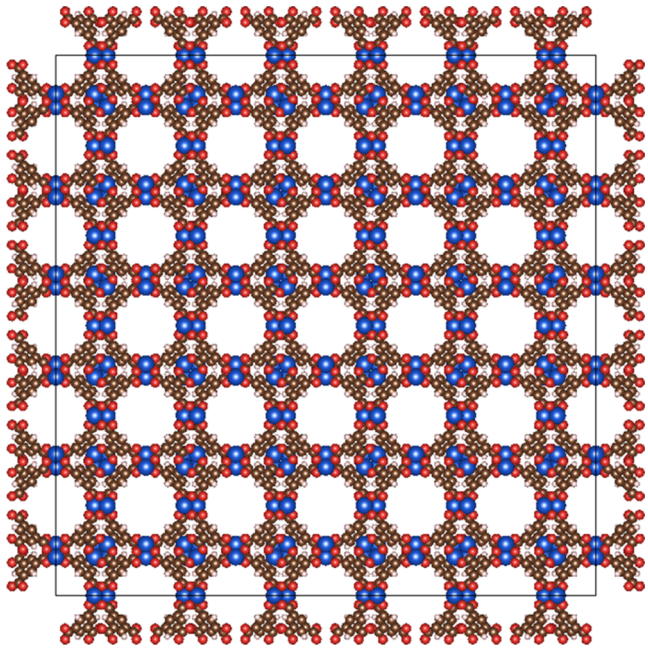

Figure 1. Front view of the HKUST-1 framework (3 × 3 × 3 supercell). The color scheme for the atoms is as follows: carbon (brown), hydrogen (white), oxygen (red), and copper (blue).

There are 864 organic linkers (H_3BTC) in the HKUST-1 (3 × 3 × 3 supercell) system. The linkers with and without defect

https://dx.doi.org/10.1021/acsami.0c16127
ACS Appl. Mater. Interfaces 2020, 12, 56172−56177

are illustrated in Figure 2a,b, respectively. We added three hydrogens after the linker removal to terminate the bonds with formate.

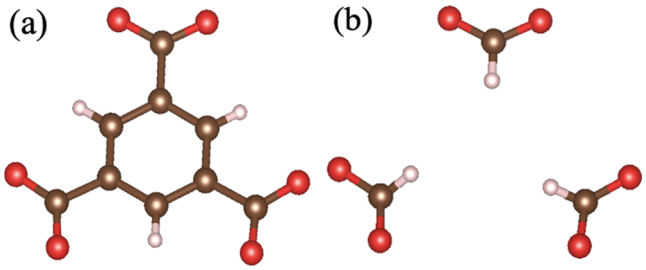

Figure 2. H_3BTC organic linkers: (a) before linker removal and (b) after linker removal. The color scheme for the atoms is as follows: carbon (brown), hydrogen (white), and oxygen (red).

To investigate the effect of defect concentrations on the thermal conductivity, we considered missing linker defect concentrations ranging from 0 to 50% in 1% increments between 0 and 5%, and in 5% increments between 5 and 50%. We also considered the effect of single linker removal, which corresponds to ∼0.11% defect concentration.

For each defect density, the thermal conductivity was obtained by averaging the respective thermal conductivities of three independent randomly generated defective structures. Various defective HKUST-1 structures are illustrated in Figure 3. Interestingly, none of HKUST-1 defective frameworks collapsed during their MD simulations, even when at defect concentrations of 50%.

RESULTS AND DISCUSSION

As can be seen in Figure 4, the thermal conductivity of HKUST-1 decreases as the missing linker defect concentration increases. Such a decrease in the thermal conductivity could be due to increased phonon-defect scattering in the framework. Figure 4 illustrates that there is a sharp drop of thermal conductivity from the pristine case to 5% defect density, which indicates that the impact of missing linker defect scattering is quite strong, leading to a substantial decrease in the thermal conductivity even at lower defect densities.

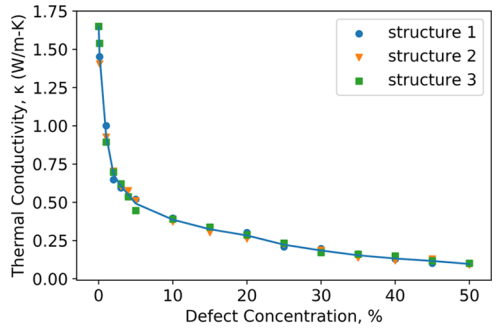

Figure 4. Thermal coductivity of HKUST-1 (3 × 3 × 3 supercell) as a function of defect concentration (blue line shows the average of thermal conductivities of three corresponding defective structures).

If we compare the thermal conductivity dependency of HKUST-1 on defect concentration with a dense crystal system such as crystalline silicon[42,53] at the same temperature (300 K), we find that the trend is the same although less pronounced for the metal−organic framework. At 1% defect concentration, the ratio of thermal conductivities between the defective and pristine case is about 0.07 for crystalline Si and 0.57 for HKUST-1. The thermal conductivity drop is an order of magnitude higher for crystalline silicon than for HKUST-1. The difference could be because of the porous nature of the HKUST-1 system compared to the densely packed structure of Si. Furthermore, the intrinsic phonon lifetime in crystalline Si[42,53] could be much longer than HKUST-1.[30] Therefore, introducing defects in Si has a much larger impact on phonon transport compared to HKUST-1. However, in porous perovskite oxides, a ∼3.3% oxygen vacancy concentration suppressed the thermal conductivity by 67%,[38] similar to our observed 63% drop in HKUST-1 for a 3% missing linker defect concentration. These similar conductivity reduction rates for the perovskite oxide and HKUST-1 could be because of their porous nature, even though the types of vacancies are different.

In our computational model, the pristine HKUST-1 thermal conductivity was determined to be 1.65 W m^{-1} K^{-1} at room temperature, which is in good agreement with the previous results.[29,30] The thermal conductivity decreased by nearly 70% at 5% defect concentration, whereas 1% defect density showed 40% decrease in the thermal conductivity with respect to the

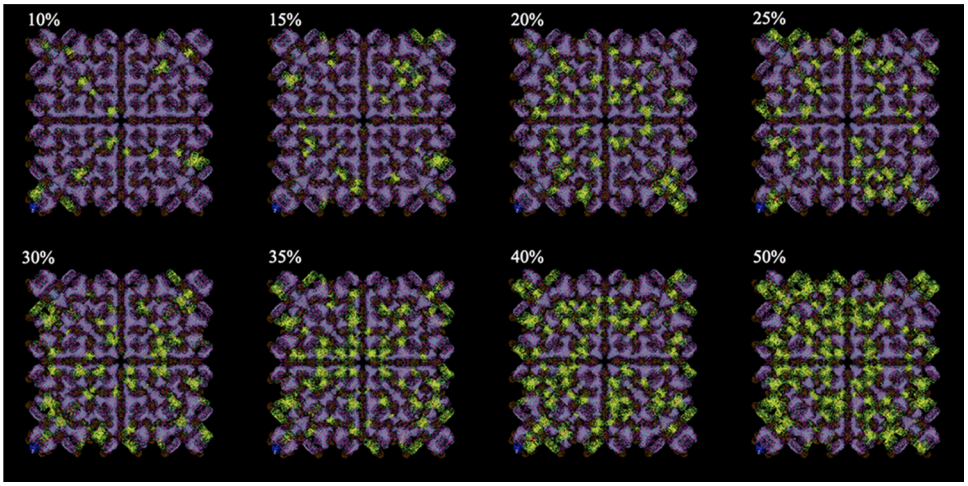

Figure 3. Front view of the HKUST-1 framework (3 × 3 × 3 supercell) supercell with various defect concentrations. Volume occupied by framework atoms depicted in blue, while volume of linkers that are missing is shown as green.

https://dx.doi.org/10.1021/acsami.0c16127
ACS Appl. Mater. Interfaces 2020, 12, 56172−56177

pristine case. Even removing only one linker from the system (corresponds to ~0.11% defect concentration) caused about 11% drop in thermal conductivity. It seems that most of the effects of missing linker defects on thermal conductivity are seen below the 5% concentration mark, after which the reduction plateaus.

Surprisingly, the spatial arrangement of the defect sites did not have much effect on the thermal conductivity, as could be seen in Figure 4, where all three structures, each corresponding to a different random arrangement of defects, mostly share very similar thermal conductivity values. Put another way, we find that the defect concentration has a stronger impact on thermal conductivity than the spatial arrangement of defects in the framework.

According to Matthiessen's rule, assuming that phonon−phonon scattering and phonon-defect scattering are independent, the effective phonon mean-free path, l_{eff}, can be expressed as[54]

$$\frac{1}{l_{eff}} = \frac{1}{l_{ph-ph}} + \frac{1}{l_p} \tag{2}$$

where l_{eff} is the effective phonon mean-free path, l_{ph-ph} is the phonon−phonon scattering length, and l_p is the phonon-defect scattering length. Mean phonon means free path is temperature-dependent and is decreased because of the scattering of phonons caused by point defects. While assuming that the thermal conductivity is proportional to the effective mean phonon free path, the thermal conductivity can be defined as

$$\frac{1}{k} \propto \frac{1}{l_{eff}} = \frac{1}{l_{ph-ph}} + \frac{1}{l_p} \tag{3}$$

Figure 5 shows that the inverse of thermal conductivity is nearly linearly dependent on the defect concentration, which

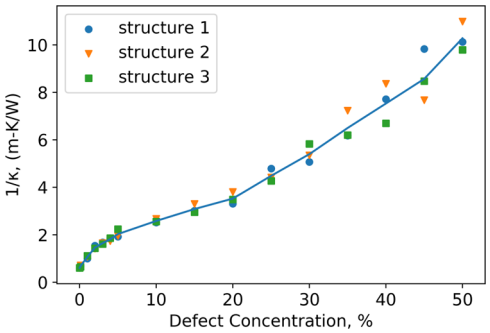

Figure 5. Inverse of thermal conductivity of HKUST-1 (3 × 3 × 3 supercell) as a function of defect concentration (blue line shows the average of thermal conductivities of three corresponding defective structures).

implies that as the missing linker concentration increases, the thermal resistivity contributed by phonon-defect scattering increases, which will result in the reduction of effective thermal conductivity.

According to the classical phonon-gas model, the thermal conductivity expression is given by[55]

$$k = \frac{1}{3} C_V v_g l_{eff}$$

where C_V is the volumetric heat capacity and v_g is the group velocity. As we remove organic linkers from the system, the density changes since the volume of the simulation box was kept constant. Assuming that all modes are fully excited, the heat capacity changes linearly with the atomic density. Consequently, it could also be possible that the thermal conductivity reduction is due to the change in the volumetric heat capacity, C_V. However, when we remove 5% of the linkers from the system, the density, and hence the volumetric heat capacity, decreases by only 1.5%. However, as we stated above, the same 5% defect density causes a 70% reduction of the thermal conductivity. Thus, we believe that the thermal conductivity change is mainly due to the phonon-defect scattering. At higher defect concentrations, the impact of heat capacity changes could be notable (50% defect density corresponds to a ~15% change in density), which could be the reason of the imperfect linear behavior of the curve in Figure 5. Although we cannot disregard the potential influence of changes in group velocity on thermal conductivity, it is unlikely that the small changes in density would dramatically alter the group velocity of the phonons. In other words, at a smaller concentration of defects (<5%), even though the effect of the heat capacity and the group velocity is not negligible, substantial changes to the thermal conductivity are mainly due to the increase of phonon-defect scattering.

Furthermore, we assume that upon removing linkers, anharmonic interactions within remaining framework atoms do not significantly change. Therefore, we believe that the sharp drop in the thermal conductivity could be mainly ascribed to the impact of increased phonon-defect scattering rather than phonon−phonon scattering. With that being said, we do not ignore the potential influence of the changes in the phonon−phonon scattering to the thermal conductivity changes observed in the study.

Our observations could potentially explain discrepancies in measured thermal conductivity values among MOFs in the literature, as defect concentrations are usually unknown and difficult to control, but where apparently small differences can have outsized impacts on the thermal conductivity. Our results also suggest that measuring thermal conductivity could potentially be a useful method for characterizing defect concentrations, particularly for MOFs that are expected to be nearly defect free.

Finally, to the extent that defect concentration can be varied intentionally, the introduction of defects (or careful prevention of defects) can be an effective strategy in tuning the thermal conductivity of HKUST-1 and other similar MOF systems.

CONCLUSIONS

We investigated the effect of missing linker defect concentration on the thermal conductivity of the HKUST-1 framework at room temperature using the classical MD simulation and the equilibrium Green−Kubo method. Defect concentrations of up to 50% were considered. These defects were introduced in various random spatial arrangements, and the resulting thermal conductivities were averaged across those configurations. It was shown that even small defect concentrations (<5%) had a substantial impact on the thermal conductivity. The defect density of even 1% displayed 40% reduction in the thermal conductivity. It was also shown that the inverse of thermal conductivity was nearly linearly dependent on defect concentration. Based on this, we believe that the reduction in the thermal conductivity could be due to increased phonon-defect scattering. Defect concentrations of up to 5% were responsible for a significant reduction (by

https://dx.doi.org/10.1021/acsami.0c16127
ACS Appl. Mater. Interfaces 2020, 12, 56172−56177

~70%) of thermal conductivity. These results could be a possible explanation for the discrepancy in the thermal conductivity values obtained experimentally and computationally for the same MOF structures (in cases where the computational model assumes a perfect defect-free crystal). Similarly, reports of measured thermal conductivities of MOFs that do not consider the presence of defects could potentially be in error.

Finally, we note that characterization of defects, both their density and their type, is notoriously difficult in MOFs, and that perhaps the thermal conductivity sensitivity observed here could be used in the future to better understand the number of defect sites in MOFs.

■ ASSOCIATED CONTENT

Supporting Information

The Supporting Information is available free of charge at https://pubs.acs.org/doi/10.1021/acsami.0c16127.

Plots of HCACF and thermal conductivity as a function of correlation time; python script to introduce defects in HKUST-1 (3 × 3 × 3 supercell) and renumber atoms and bond lists (PDF)

PythonScripts (ZIP)

■ AUTHOR INFORMATION

Corresponding Author

Christopher E. Wilmer − *Department of Chemical & Petroleum Engineering and Department of Electrical & Computer Engineering, University of Pittsburgh, Pittsburgh, Pennsylvania 15261, Unites States;* orcid.org/0000-0002-7440-5727; Email: wilmer@pitt.edu

Authors

Meiirbek Islamov − *Department of Chemical & Petroleum Engineering, University of Pittsburgh, Pittsburgh, Pennsylvania 15261, Unites States*

Hasan Babaei − *Department of Chemistry, University of California-Berkeley, Berkeley, California 94720, United States;* orcid.org/0000-0002-3291-0290

Complete contact information is available at: https://pubs.acs.org/10.1021/acsami.0c16127

Author Contributions

The manuscript was written through the contributions of all authors. All authors have given approval to the final version of the manuscript.

Notes

The authors declare the following competing financial interest(s): Christopher E. Wilmer has a financial interest in the start-up company NuMat Technologies, which is seeking to commercialize metal-organic frameworks.

■ ACKNOWLEDGMENTS

M.I., H.B., and C.E.W. gratefully acknowledge support from the National Science Foundation (NSF), awards CBET-1804011 and OAC-1931436, and also thank the Center for Research Computing (CRC) at the University of Pittsburgh for providing computational resources.

■ REFERENCES

(1) Zhou, H.-C. "Joe".; Kitagawa, S. Metal−Organic Frameworks (MOFs). *Chem. Soc. Rev.* **2014**, *43*, 5415−5418.

(2) Yaghi, O. M.; O'Keeffe, M.; Ockwig, N. W.; Chae, H. K.; Eddaoudi, M.; Kim, J. Reticular Synthesis and the Design of New Materials. *Nature* **2003**, *423*, 705−714.

(3) Furukawa, H.; Müller, U.; Yaghi, O. M. "Heterogeneity within Order" in Metal-Organic Frameworks. *Angew. Chem., Int. Ed.* **2015**, *54*, 3417−3430.

(4) Rosi, N. L. Hydrogen Storage in Microporous Metal-Organic Frameworks. *Science* **2003**, *300*, 1127−1129.

(5) Furukawa, H.; Cordova, K. E.; O'Keeffe, M.; Yaghi, O. M. The Chemistry and Applications of Metal-Organic Frameworks. *Science* **2013**, *341*, No. 1230444.

(6) Mason, J. A.; Veenstra, M.; Long, J. R. Evaluating Metal−Organic Frameworks for Natural Gas Storage. *Chem. Sci.* **2014**, *5*, 32−51.

(7) He, Y.; Zhou, W.; Qian, G.; Chen, B. Methane Storage in Metal−Organic Frameworks. *Chem. Soc. Rev.* **2014**, *43*, 5657−5678.

(8) Sumida, K.; Rogow, D. L.; Mason, J. A.; McDonald, T. M.; Bloch, E. D.; Herm, Z. R.; Bae, T.-H.; Long, J. R. Carbon Dioxide Capture in Metal−Organic Frameworks. *Chem. Rev.* **2012**, *112*, 724−781.

(9) Li, J.-R.; Kuppler, R. J.; Zhou, H.-C. Selective Gas Adsorption and Separation in Metal−Organic Frameworks. *Chem. Soc. Rev.* **2009**, *38*, 1477.

(10) Qiu, S.; Xue, M.; Zhu, G. Metal−Organic Framework Membranes: From Synthesis to Separation Application. *Chem. Soc. Rev.* **2014**, *43*, 6116−6140.

(11) Kreno, L. E.; Leong, K.; Farha, O. K.; Allendorf, M.; Van Duyne, R. P.; Hupp, J. T. Metal−Organic Framework Materials as Chemical Sensors. *Chem. Rev.* **2012**, *112*, 1105−1125.

(12) Hu, Z.; Deibert, B. J.; Li, J. Luminescent Metal−Organic Frameworks for Chemical Sensing and Explosive Detection. *Chem. Soc. Rev.* **2014**, *43*, 5815−5840.

(13) Lee, J.; Farha, O. K.; Roberts, J.; Scheidt, K. A.; Nguyen, S. T.; Hupp, J. T. Metal−Organic Framework Materials as Catalysts. *Chem. Soc. Rev.* **2009**, *38*, 1450.

(14) Liu, J.; Chen, L.; Cui, H.; Zhang, J.; Zhang, L.; Su, C.-Y. Applications of Metal−Organic Frameworks in Heterogeneous Supramolecular Catalysis. *Chem. Soc. Rev.* **2014**, *43*, 6011−6061.

(15) Zhang, T.; Lin, W. Metal−Organic Frameworks for Artificial Photosynthesis and Photocatalysis. *Chem. Soc. Rev.* **2014**, *43*, 5982−5993.

(16) Mueller, U.; Schubert, M.; Teich, F.; Puetter, H.; Schierle-Arndt, K.; Pastré, J. Metal−Organic Frameworks—Prospective Industrial Applications. *J. Mater. Chem.* **2006**, *16*, 626−636.

(17) Zhang, H.; Deria, P.; Farha, O. K.; Hupp, J. T.; Snurr, R. Q. A Thermodynamic Tank Model for Studying the Effect of Higher Hydrocarbons on Natural Gas Storage in Metal−Organic Frameworks. *Energy Environ. Sci.* **2015**, *8*, 1501−1510.

(18) Huang, B. L.; McGaughey, A. J. H.; Kaviany, M. Thermal Conductivity of Metal-Organic Framework 5 (MOF-5): Part I. Molecular Dynamics Simulations. *Int. J. Heat Mass Transfer* **2007**, *50*, 393−404.

(19) Huang, B. L.; Ni, Z.; Millward, A.; McGaughey, A. J. H.; Uher, C.; Kaviany, M.; Yaghi, O. Thermal Conductivity of a Metal-Organic Framework (MOF-5): Part II. Measurement. *Int. J. Heat Mass Transfer* **2007**, *50*, 405−411.

(20) Liu, D.; Purewal, J. J.; Yang, J.; Sudik, A.; Maurer, S.; Mueller, U.; Ni, J.; Siegel, D. J. MOF-5 Composites Exhibiting Improved Thermal Conductivity. *Int. J. Hydrogen Energy* **2012**, *37*, 6109−6117.

(21) Zhang, X.; Jiang, J. Thermal Conductivity of Zeolitic Imidazolate Framework-8: A Molecular Simulation Study. *J. Phys. Chem. C* **2013**, *117*, 18441−18447.

(22) Wang, X.; Guo, R.; Xu, D.; Chung, J.; Kaviany, M.; Huang, B. Anisotropic Lattice Thermal Conductivity and Suppressed Acoustic Phonons in MOF-74 from First Principles. *J. Phys. Chem. C* **2015**, *119*, 26000−26008.

(23) Babaei, H.; McGaughey, A. J. H.; Wilmer, C. E. Transient Mass and Thermal Transport during Methane Adsorption into the Metal−

Organic Framework HKUST-1. *ACS Appl. Mater. Interfaces* **2018**, *10*, 2400−2406.
(24) Ming, Y.; Purewal, J.; Liu, D.; Sudik, A.; Xu, C.; Yang, J.; Veenstra, M.; Rhodes, K.; Soltis, R.; Warner, J.; Gaab, M.; Müller, U.; Siegel, D. J. Thermophysical Properties of MOF-5 Powders. *Microporous Mesoporous Mater.* **2014**, *185*, 235−244.
(25) Cui, B.; Audu, C. O.; Liao, Y.; Nguyen, S. T.; Farha, O. K.; Hupp, J. T.; Grayson, M. Thermal Conductivity of ZIF-8 Thin-Film under Ambient Gas Pressure. *ACS Appl. Mater. Interfaces* **2017**, *9*, 28139−28143.
(26) Sezginel, K. B.; Lee, S.; Babaei, H.; Wilmer, C. E. Effect of Flexibility on Thermal Transport in Breathing Porous Crystals. *J. Phys. Chem. C* **2020**, *124*, 18604−18608.
(27) Sezginel, K. B.; Asinger, P. A.; Babaei, H.; Wilmer, C. E. Thermal Transport in Interpenetrated Metal−Organic Frameworks. *Chem. Mater.* **2018**, *30*, 2281−2286.
(28) Babaei, H.; McGaughey, A. J. H.; Wilmer, C. E. Effect of Pore Size and Shape on the Thermal Conductivity of Metal-Organic Frameworks. *Chem. Sci.* **2017**, *8*, 583−589.
(29) Babaei, H.; Wilmer, C. E. Mechanisms of Heat Transfer in Porous Crystals Containing Adsorbed Gases: Applications to Metal-Organic Frameworks. *Phys. Rev. Lett.* **2016**, *116*, No. 025902.
(30) Babaei, H.; DeCoster, M. E.; Jeong, M.; Hassan, Z. M.; Islamoglu, T.; Baumgart, H.; McGaughey, A. J. H.; Redel, E.; Farha, O. K.; Hopkins, P. E.; Malen, J. A.; Wilmer, C. E. Observation of Reduced Thermal Conductivity in a Metal-Organic Framework Due to the Presence of Adsorbates. *Nat. Commun.* **2020**, *11*, No. 4010.
(31) Sholl, D. S.; Lively, R. P. Defects in Metal−Organic Frameworks: Challenge or Opportunity? *J. Phys. Chem. Lett.* **2015**, *6*, 3437−3444.
(32) Dissegna, S.; Epp, K.; Heinz, W. R.; Kieslich, G.; Fischer, R. A. Defective Metal-Organic Frameworks. *Adv. Mater.* **2018**, *30*, No. 1704501.
(33) Diring, S.; Furukawa, S.; Takashima, Y.; Tsuruoka, T.; Kitagawa, S. Controlled Multiscale Synthesis of Porous Coordination Polymer in Nano/Micro Regimes. *Chem. Mater.* **2010**, *22*, 4531−4538.
(34) Vermoortele, F.; Bueken, B.; Le Bars, G.; Van de Voorde, B.; Vandichel, M.; Houthoofd, K.; Vimont, A.; Daturi, M.; Waroquier, M.; Van Speybroeck, V.; Kirschhock, C.; De Vos, D. E. Synthesis Modulation as a Tool To Increase the Catalytic Activity of Metal−Organic Frameworks: The Unique Case of UiO-66(Zr). *J. Am. Chem. Soc.* **2013**, *135*, 11465−11468.
(35) Wu, H.; Chua, Y. S.; Krungleviciute, V.; Tyagi, M.; Chen, P.; Yildirim, T.; Zhou, W. Unusual and Highly Tunable Missing-Linker Defects in Zirconium Metal−Organic Framework UiO-66 and Their Important Effects on Gas Adsorption. *J. Am. Chem. Soc.* **2013**, *135*, 10525−10532.
(36) Vermoortele, F.; Ameloot, R.; Alaerts, L.; Matthessen, R.; Carlier, B.; Fernandez, E. V. R.; Gascon, J.; Kapteijn, F.; De Vos, D. E. Tuning the Catalytic Performance of Metal−Organic Frameworks in Fine Chemistry by Active Site Engineering. *J. Mater. Chem.* **2012**, *22*, 10313.
(37) Ravon, U.; Savonnet, M.; Aguado, S.; Domine, M. E.; Janneau, E.; Farrusseng, D. Engineering of Coordination Polymers for Shape Selective Alkylation of Large Aromatics and the Role of Defects. *Microporous Mesoporous Mater.* **2010**, *129*, 319−329.
(38) Wu, X.; Walter, J.; Feng, T.; Zhu, J.; Zheng, H.; Mitchell, J. F.; Biškup, N.; Varela, M.; Ruan, X.; Leighton, C.; Wang, X. Glass-Like Through-Plane Thermal Conductivity Induced by Oxygen Vacancies in Nanoscale Epitaxial $La_{0.5}Sr_{0.5}CoO_{3-\delta}$. *Adv. Funct. Mater.* **2017**, *27*, No. 1704233.
(39) Noshin, M.; Khan, A. I.; Navid, I. A.; Uddin, H. M. A.; Subrina, S. Impact of Vacancies on the Thermal Conductivity of Graphene Nanoribbons: A Molecular Dynamics Simulation Study. *AIP Adv.* **2017**, *7*, No. 015112.
(40) Bouzerar, G.; Thébaud, S.; Pecorario, S.; Adessi, C. Drastic Effects of Vacancies on Phonon Lifetime and Thermal Conductivity in Graphene. *J. Phys.: Condens. Matter* **2020**, *32*, No. 295702.
(41) Yarali, M.; Brahmi, H.; Yan, Z.; Li, X.; Xie, L.; Chen, S.; Kumar, S.; Yoon, M.; Xiao, K.; Mavrokefalos, A. Effect of Metal Doping and Vacancies on the Thermal Conductivity of Monolayer Molybdenum Diselenide. *ACS Appl. Mater. Interfaces* **2018**, *10*, 4921−4928.
(42) Lee, Y.; Lee, S.; Hwang, G. S. Effects of Vacancy Defects on Thermal Conductivity in Crystalline Silicon: A Nonequilibrium Molecular Dynamics Study. *Phys. Rev. B* **2011**, *83*, No. 125202.
(43) Protik, N. H.; Carrete, J.; Katcho, N. A.; Mingo, N.; Broido, D. *Ab Initio* Study of the Effect of Vacancies on the Thermal Conductivity of Boron Arsenide. *Phys. Rev. B* **2016**, *94*, No. 045207.
(44) Seyf, H. R.; Yates, L.; Bougher, T. L.; Graham, S.; Cola, B. A.; Detchprohm, T.; Ji, M.-H.; Kim, J.; Dupuis, R.; Lv, W.; Henry, A. Rethinking Phonons: The Issue of Disorder. *npj Comput. Mater.* **2017**, *3*, No. 49.
(45) Garg, J.; Bonini, N.; Kozinsky, B.; Marzari, N. Role of Disorder and Anharmonicity in the Thermal Conductivity of Silicon-Germanium Alloys: A First-Principles Study. *Phys. Rev. Lett.* **2011**, *106*, No. 045901.
(46) Shiomi, J.; Esfarjani, K.; Chen, G. Thermal Conductivity of Half-Heusler Compounds from First-Principles Calculations. *Phys. Rev. B* **2011**, *84*, No. 104302.
(47) Nie, J.; Ranganathan, R.; Liang, Z.; Keblinski, P. Structural vs. Compositional Disorder in Thermal Conductivity Reduction of SiGe Alloys. *J. Appl. Phys.* **2017**, *122*, No. 045104.
(48) Sørensen, S. S.; Østergaard, M. B.; Stepniewska, M.; Johra, H.; Yue, Y.; Smedskjaer, M. M. Metal−Organic Framework Glasses Possess Higher Thermal Conductivity than Their Crystalline Counterparts. *ACS Appl. Mater. Interfaces* **2020**, *12*, 18893−18903.
(49) Chui, S. S. A Chemically Functionalizable Nanoporous Material [Cu3(TMA)2(H2O)3]n. *Science* **1999**, *283*, 1148−1150.
(50) Babaei, H.; Keblinski, P.; Khodadadi, J. M. Equilibrium Molecular Dynamics Determination of Thermal Conductivity for Multi-Component Systems. *J. Appl. Phys.* **2012**, *112*, No. 054310.
(51) Plimpton, S. Fast Parallel Algorithms for Short-Range Molecular Dynamics. *J. Comput. Phys.* **1995**, *117*, 1−19.
(52) Zhao, L.; Yang, Q.; Ma, Q.; Zhong, C.; Mi, J.; Liu, D. A Force Field for Dynamic Cu-BTC Metal-Organic Framework. *J. Mol. Model.* **2011**, *17*, 227−234.
(53) Babaei, H.; Guo, R.; Hashemi, A.; Lee, S. Machine-Learning-Based Interatomic Potential for Phonon Transport in Perfect Crystalline Si and Crystalline Si with Vacancies. *Phys. Rev. Mater.* **2019**, *3*, No. 074603.
(54) McGaughey, A. J. H.; Jain, A. Nanostructure Thermal Conductivity Prediction by Monte Carlo Sampling of Phonon Free Paths. *Appl. Phys. Lett.* **2012**, *100*, No. 061911.
(55) Srivastava, G. P. *The Physics of Phonons*; A. Hilger: Bristol; Philadelphia, 1990.

https://dx.doi.org/10.1021/acsami.0c16127
ACS Appl. Mater. Interfaces 2020, 12, 56172−56177